Processing and Characterization of Free Standing Highly Oriented Ferroelectric Polymer Films with Remarkably Low Coercive Field and High Remnant Polarization

Nan Meng [1], Rui Mao [1], Wei Tu [2], Xiaojing Zhu [1],Rory M. Wilson [1], Emiliano Bilotti [1, 2], Michael J. Reece [1, 2]*

[1] School of Engineering and Materials Science, and Materials Research Institute, Queen Mary University of London, Mile End Road, E1 4NS London, UK

[2] Nanoforce Technology Ltd., Joseph Priestley Building, Queen Mary University of London, Mile End Road, E1 4NS London, UK

Queen Mary University of London,

School of Engineering and Materials Science,

Mile End Road E1 4NS, London, UK

Tel: +44 (0)20 7882 8872; E-mail: m.j.reece@qmul.ac.uk

Key words: PVDF-TrFE; Oriented; Ferroelectric properties

Abstract: Highly aligned poly(vinylidene fluoride-co-trifluoroethylene) (PVDF-TrFE) films were processed using a scalable one-step melt extrusion processing route. Crystalline structure and orientation were optimized by controlling the melt extrusion conditions. XRD patterns suggested the nearly perfect alignment of the c-axis (polymer chain direction) along the extrusion direction in the optimized as-extruded films. SEM analysis confirmed the morphology of the crystalline phase, showing edge-on lamellae stacked perpendicular to the extrusion direction. DSC data indicated high crystallinity and well-ordered ferroelectric structure of the extruded films. The FTIR spectroscopy proved strong intermolecular dipole-dipole interaction in the extruded films. Accordingly, the optimized as-extruded PVDF-TrFE films exhibit a coercive field of 24 kV/mm, half of the commonly reported values for bulk films (~50 kV/mm) and a remnant polarization of 0.078 C/m^2 which further increased to

0.099 C/m^2 after annealing. This value is close to the theoretical limit (0.102 C/m^2) assuming perfect in-plane c-axis orientation and 100% crystallinity.

1. Introduction

Ferroelectric polymers, poly(vinylidene fluoride) (PVDF) and its copolymer poly(vinylidene fluoride-co-trifluoroethylene) (PVDF-TrFE) are promising candidate materials for the application in flexible organic electronic devices; for instance, organic solar cells[1], lithium-ion batteries[2], non-volatile memories[3,4] and piezoelectric sensors[5]. The minimum working voltage for devices based on the ferroelectric properties is influenced by the coercive field (E_c). The E_c of ferroelectric polymers is an order of magnitude larger than common ferroelectric inorganic oxides, which is about 50 kV/mm for PVDF and PVDF-TrFE.[6, 7] A high remnant polarization (P_r) is desirable for the performance of devices, which is significantly related to the crystallization of ferroelectric polymers. Low crystallinity results in a severe decline of P_r. Moreover, the common solution processing methods are multi-step, time-consuming and not industrial favourable. The high E_c, low P_r and not scalable processing routes are the main bottlenecks hindering the application of ferroelectric polymers.

PVDF has a complex crystallization nature; at least four polymorphs (α-, β-, γ-, and δ-phase) have been confirmed, among which the most energetically favourable phase is the non-polar α-phase, with trans-gauche chain conformation[8], while the β-phase, with trans-trans chain conformation, is ferroelectric with its polar direction along its b-axis. Post-treatments are required, either mechanical stretching or poling at high electric field (>500 KV/mm), to obtain the ferroelectric β phase in PVDF.[9] With regard to PVDF-TrFE, its chain configuration and crystalline structure are composition dependent.[10-13] PVDF-TrFE with 50-80 mol. % VDF has an all-trans chain conformation and crystallizes into the ferroelectric phase without post-treatments.[6] Moreover, PVDF-TrFE with 50-80 mol. % VDF exhibits an obvious Curie transition. In terms of the Curie transition, the different crystalline phases of PVDF-TrFE are notated as low temperature phase (LT), high temperature phase (HT) and cooled phase (CL). The LT phase is essentially the same as that of the β-phase[14,15] and transforms into the HT phase above the Curie point. The HT phase contains large amounts of gauche bonds, and can be considered as a mixture of the γ- and α-phases.[15] The CL phase is obtained by slowly cooling the HT phase. Compared to the LT phase, the CL phase is less regular and transforms into the LT phase by stretching or poling.[15] In comparison with PVDF,

the much easier crystallization into ferroelectric phase makes PVDF-TrFE more attractive in the application field.

The crystallographic structure of PVDF-TrFE ferroelectric LT phase is orthorhombic unit cell in which the values of a-, b-, and c- are 9.05 Å, 5.12 Å and 2.55 Å (PVDF-TrFE 70/30 mol. %[16]). The ferroelectric properties are generated from the permanent dipoles with the spontaneous polarization (P_s) along the b-axis. The ferroelectric switching is accomplished by the coupling global rotation of molecular polymer chain axis (c-axis).[8,17,18] The P_s value is intrinsic and solely dependent on the crystal structure, while the remnant polarization P_r is linked to the degree of crystallinity and orientation of the c-axis. If the c-axis is perfectly oriented in the film plane and the b-axis about the c-axis is random, the maximum possible value (100% crystalline) of P_r is 95% of P_s.[6] Therefore, good in-plane c-axis orientation and high crystallinity are required to achieve a high P_r value.

The coercive field E_c corresponds to the electric field at which the net polarization of a material is zero and the maximum rate of ferroelectric switching occurs[19]. Experimental values of E_c for most ferroelectrics are a few orders of magnitude lower than the theoretically predicted Landau–Ginzburg (LG) intrinsic E_c.[20] In the LG model the E_c corresponds to the electric field needed to overcome the minimum of free Gibbs energy density.[20] The LG intrinsic E_c value of PVDF-TrFE is ~600 kV/mm,[20] but the typically measured E_c values are ~50 kV/mm.[21-23] The much lower experimentally measured values are due to the actual mechanism of nucleation of ferroelectric domains which involves the localized nucleation of domains followed by the forward and sideways growth.[24] Under this mechanism the domain nucleation normally occurs at defects/imperfections. Apart from acting as the domain nucleation agents, defects/imperfections also serve as pinning sites during the domain wall movement and thereby hindering the subsequent growth of domains.[24,25] Consequently, the E_c for ferroelectrics is an extrinsic value and importantly dependent on the degree of crystallographic order/perfection. The semi-crystalline nature and unavoidably irregular polymer crystals and the crystalline orientation of PVDF-TrFE escalate the complexity of its ferroelectric polarization reversal.[24]

The way a polymer is processed can significantly influence crystalline orientation, degree of crystallinity, as well as the crystalline phases formed.

Melt extrusion is a common method used to produce oriented flexible chain polymers. Plenty of studies [26-32] related to melt extrusion has been conducted on polyethylene (PE) which has

the same all-trans chain conformation as that of PVDF-TrFE (50-80 mol. % VDF), giving rise to a similar crystallographic structure; orthorhombic unit cell in which the values of a-, b-, and c- are 7.4 Å, 4.94 Å and 2.54 Å[30]. Under high axial directed stress well-stacked untwisted lamellae crystallites are formed in PE as well as a preferred orientation of the c-axis along the stress direction (c-texture).[28] With regard to PVDF-TrFE extruded films, Furukawa[23] reported the PVDF-TrFE 78/22 mol. % extruded films exhibited a sharp switching current peak due to the well-aligned lamellae, but the characterization of crystalline orientation and the E_c value were not reported and the P_r of as-extruded films was only 0.03 C/m^2. Lovinger *et al.* [33] reported extruded PVDF-TrFE 52/48 mol. % films poled at 70 kV/mm at room temperature showed preferred orientation, which they assumed was produced by the poling and not the extrusion.

In this contribution, we firstly proved the clear preferred orientation of the extruded PVDF-TrFE films using a similar composition material 51/49 mol. % (Figure S1). Then we determined the optimum processing temperature and produced free standing highly oriented ferroelectric PVDF-TrFE films using melt extrusion. The E_c of highly oriented films was 24 kV/mm, which is half of the commonly reported value for bulk films (50 KV/mm). The P_r of the annealed optimized extruded films 0.099 C/m^2 reached to the theoretical limit 0.102 C/m^2.

2. Experimental details

2.1 Materials

PVDF-TrFE pellets, with the molecular composition of 77/23 mol% were purchased from Piezotech S.A.S, (France). The molecular weights reported by other researchers are Mw and Mn 210 and 100 kg/mol, respectively.[34]

2.2 Sample preparation

The PVDF-TrFE was melt-processed using a 15 ml X'plore micro compounder (MC 15) and then collected using an X'plore micro cast film line (Xplore Instruments, Geleen, The Netherlands). The extrusion temperature was set at 170℃, 175 ℃, 190 ℃, 205 ℃ or 210 ℃. The screw speed was 75 rpm. A 200 μm slit die was connected to the extruder. The take up speed was 180 mm/min at ambient conditions. Films extruded at 190 ℃ were clamped and annealed at 140 ℃ for 24 hours. The thickness of extruded films was roughly about 10-35 μm.

For ferroelectric measurements, gold electrodes (~ 100 nm thick, 2 mm diameter) were evaporated on both sides of the films.

2.3 Characterization

The crystalline structure and preferred orientation were characterized by two-dimensional wide-angle X-ray diffraction (2D-WAXD) ring patterns which were obtained using transmission geometry on a single crystal X-ray diffractometer (Kappa ApexII Duo, Bruker AXS GmbH, Karlsruhe, Germany) with the incident beam either normal to the film surface or parallel to the extrusion direction. The 2D-WAXD ring patterns were analysed using FIT 2D software (European Synchrotron Radiation Facility, Grenoble, France) to obtain the azimuthal intensity plots, which were fitted using a Gaussian function. The Herman's orientation factor (*f*) calculated from the Gaussian fitting plots was used to quantitatively determine the degree of preferred orientation. Equation (1) describes the calculation of *f*; φ denotes the angle between the chain axis and the reference direction. If all of the polymer chains are ideally oriented along the reference direction, then φ= 0° and *f*= 1. On the contrary, if all polymer chains are perpendicularly oriented with respect to the reference direction, then φ= 90° and *f*= -1/2. In the case of random orientation, *f* will be equal to 0. In this work, the extrusion direction was chosen as the reference direction.

$$f = (3 \langle cos^2\varphi \rangle - 1)/2 \qquad (1)$$

Morphological studies of the gold coated films were made using scanning electron microscopy (SEM) (FEI Inspect-F, Hillsboro, OR, USA). For side and cross-section morphology, the samples were embedded in a resin. The resin blocks were pre-cracked and then cold fractured in liquid nitrogen. Samples for SEM were etched in potassium permanganate solution (0.3 M) for 30 min at 50 ℃ to remove the amorphous region. Thermodynamic parameters like Curie point (T_c), melting temperature (T_m), as well as the enthalpies of the Curie transition (ΔH_c) and fusion (ΔH_f) were determined using a differential scanning calorimetry (DSC) (DSC4000, PerkinElmer, Massachusetts, USA). All samples were heated from 25 ℃ to 180 ℃ under a N_2 atmosphere, and the heating and cooling rates were 5 ℃/ min. In order to demonstrate the effect of preferred orientation on thermal behaviour, a second heating scan after cooling was also conducted as a reference. The values of the characteristic temperature and thermodynamic parameters presented in this work are the average for 6 specimens. Fourier transform infrared spectroscopy (FTIR) (Tensor 27, Bruker Optik GmbH, Ettlingen, Germany) was used to analyse the molecular alignment. The

FTIR scans were performed with 32 scans for one sample and a resolution of 4 cm^{-1} in the wavenumber range of 4000-400 cm^{-1}.

A ferroelectric hysteresis measurement tester (NPL, Teddington, UK) was used to test ferroelectric polarization-electric field (P-E) loops at room temperature and 10 Hz.[35]

3. Results and discussions

3.1 Crystalline preferred orientation

Figure 1 shows two-dimensional wide-angle X-ray diffraction 2D-WAXD ring patterns of the PVDF-TrFE films extruded at different temperatures. In Figure 1a-e, all samples exhibit equatorial 110 and 200 reflections, suggesting that their c-axes were preferentially oriented along the extrusion direction. The corresponding diffraction angle is $2\theta = 20.12°$. The 190 ℃ extruded films had the narrowest arcs. The preferred orientation of the films was quantified using Herman's orientation factor (*f*) using a Gaussian fit. Calculated values of Herman's orientation factor (*f*) are listed at the bottom of Figure 1. For the films extruded at 170 ℃, *f* is 0.65, indicating moderate crystalline preferred orientation. It increased to 0.72 for the 175 ℃ extruded films. After peaking to 0.89 for the 190 ℃ extruded films, *f* slightly decreased to 0.81 for the 205 ℃ extruded films and further declined to 0.57 for the 210 ℃ extruded films. The change of the *f* values indicates the orientation degree of polymer chains is strongly related to the extrusion temperature and more details will be discussed later in the SEM morphology part. Figure 1f shows the diffraction pattern with X-ray beam along the extrusion direction (i.e., through the thickness of the film). The complete ring in Figure 1f indicates the random orientation of the b-axis about the c-axis in the extruded PVDF-TrFE films.

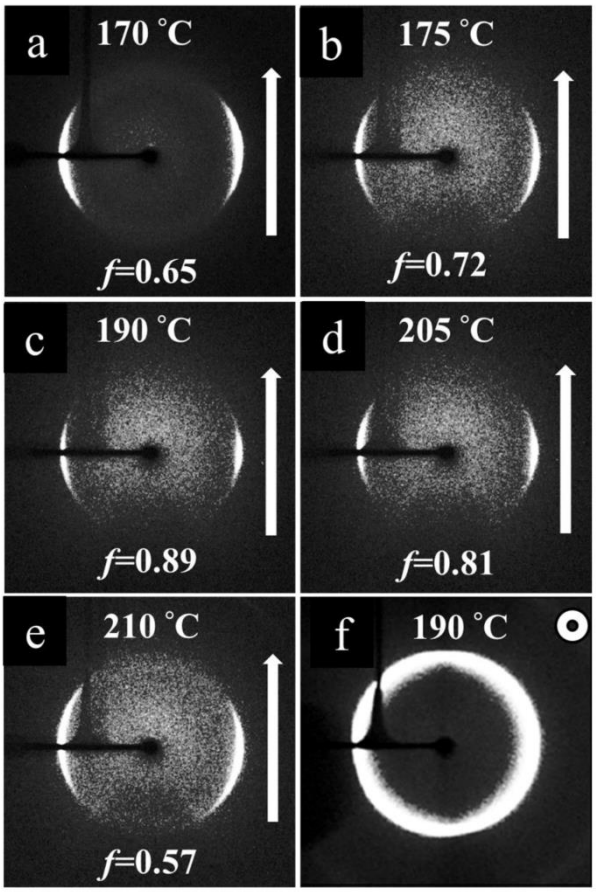

Figure 1 2D-WAXD ring patterns for PVDF-TrFE films extruded at: (a) 170 ℃; (b) 175 ℃; (c) 190 ℃; (d) 205 ℃ and (e) 210 ℃. Arrows indicate the extrusion direction, and the X-ray beam was parallel with the normal to the film surface. Values of Herman's orientation factor (*f*) are listed at the bottom. (f) 2D-WAXD ring pattern for the cross-section of PVDF-TrFE films extruded at 190 ℃, and X-ray beam was parallel to the extrusion direction.

3.2 Morphology determination

Film surface, side and cross-section SEM images were used to determine the structure of the crystallites in the 190 ℃ extruded films (Figure 2a-c). Surface morphology displayed well-ordered lamellae oriented perpendicular to the extrusion direction (Figure 2a), which is consistent with the XRD data showing the narrowest equatorial 110 and 200 reflections (Figure 1c). The side region morphology (Figure 2b) of the extruded films is similar to that displayed by the film surface, while the cross-section region (Figure 2c) along the extrusion direction exhibits a flat morphology which is consistent with the random orientation concluded from the XRD data (Figure 1f). Lamellae crystallites are formed by folded chains and grow in the direction along the largest temperature gradient which is the extrusion direction during processing. According to the XRD data (Figure 1a-e), polymer chain axes

are also along the extrusion direction. Combined these with the SEM images, the extruded PVDF-TrFE films crystallize into edge-on lamellae crystallites (as illustrated in Figure 2d). Such well-ordered edge-on lamellae is beneficial for ferroelectric polarization reversal due to the less domain wall pinning effect that arises from the more ordered structure. The cubic shape shown in Figure 2d is only for graphic simplification. As shown in Figure 2c the face side of the lamellae have polyhedral shape. The thickness of the lamellae crystallites are about 10 nm, which is consistent with calculated value using Scherrer equation on the XRD data (12 nm).

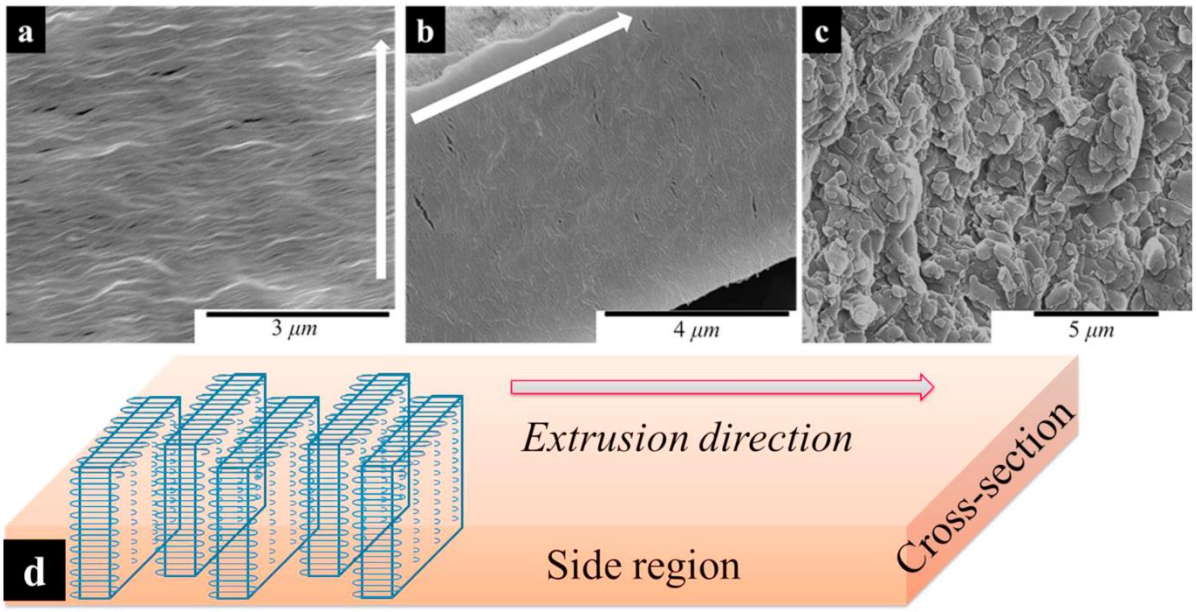

Figure 2 Structure determinations for 190 ℃ extruded films: (a) film surface SEM image; (b) side region along the extrusion direction SEM image; (c) cross-section perpendicular to the extrusion direction SEM image; and (d) corresponding schematic diagram of edge-on lamellae.

Figure 3 shows the comparison of surface morphology for PVDF-TrFE films extruded at different temperatures. When PVDF-TrFE was extruded at 170 ℃, due to its relatively high viscosity, the polymer chains were difficult to mobilize under the extension flow. As a result, the PVDF-TrFE crystallized into slightly aligned long needle-like lamellae (Figure 3a). The surface morphology changed to a twisted lamellae morphology when the extrusion temperature was increased to 175 ℃ (Figure 3b). A high proportion of the lamellae oriented perpendicular to the extrusion direction, suggesting planar extension flow along the extrusion direction and uniaxial preferred orientation. As discussed before, the 190 ℃ extruded films exhibited well-ordered lamellae oriented perpendicular to the extrusion direction (Figure 3c). The films extruded at 205 °C and 210 °C (Figure 3d and 3e) displayed more twisted or tilted

lamellae morphology compared to the film extruded at 190 °C (Figure 3c), especially the films extruded at 210 °C.

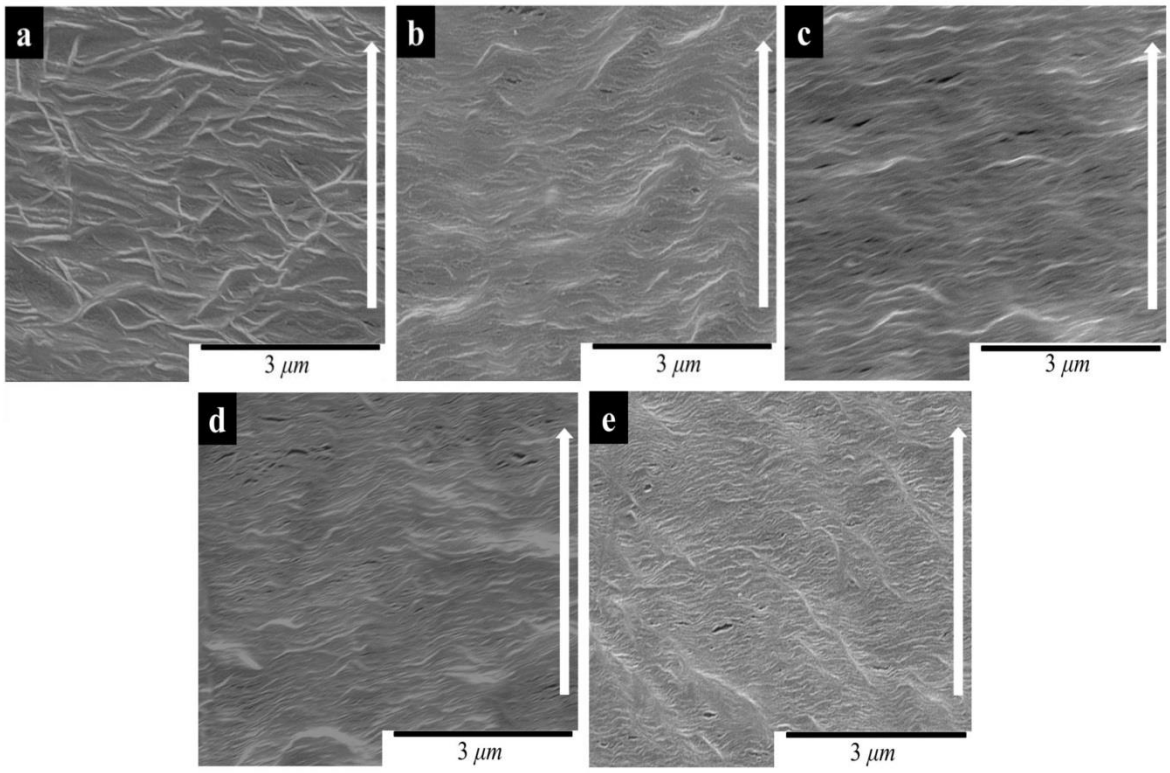

Figure 3 Surface SEM images of PVDF-TrFE extruded at different temperatures: (a) 170 ℃; (b) 175 ℃; (c) 190 ℃; (d) 205 ℃; (e) 210 ℃. Arrows indicate the extrusion direction.

At the lower extrusion temperatures (below 175 °C) the higher viscosity of the films produced longer chain relaxation times at the die exit. When the extrusion temperature was above 175 ℃, the chain mobility was high enough for extension flow. However, with further increasing temperature, shorter chain relaxation times prejudiced preferred orientation. The 170 ℃ and 210 ℃ extruded films will not be discussed further in the paper because of the much less preferred orientation compared to the other three.

3.3 Thermal analysis

Figure 4 shows the DSC first heating scans for the PVDF-TrFE films extruded at different temperatures. The characteristic temperature values and thermodynamic parameters obtained from DSC are listed in Table 1. A sample crystallized during a DSC cooling process that had not experienced extension flow was chosen as a reference. The extruded films show a higher Curie point T_c and lower melting temperature T_m compared to the reference sample. Large amounts of gauche bonds possessing higher potential energy are formed during Curie

transition. The higher T_c indicates well-ordered all-trans chains in the extruded films. The T_c increased from 132.8 to 134.0 ℃ when the extrusion temperature increased from 175 to 190 ℃. A further increase of the extrusion temperature to 205 ℃ did not make a significant difference (only 0.2 ℃ higher). Considering the morphological features of the films (Figure 3), the 190 ℃ extruded films displayed more planar lamellae texture, indicating higher preferred orientation compared to the film extruded at 175 ℃, which resulted in a higher T_c. The level of preferred orientation did not significantly alter the T_m values, and they were all at about 147.5 ℃ for the PVDF-TrFE extruded films. The higher T_m of the reference sample is ascribed to the slower cooling rate during the DSC experiments compared to the extrusion processing allowing more time to array polymer chains forming larger crystallites. Both the extrusion and reference samples showed similar fusion enthalpy ΔH_f values, which indicates that the degree of crystallinity of all of the films was similar. Koga *et al.* [36] reported the ΔH_f of PVDF-TrFE 74/26 mol. % films annealed at 140 ℃ for 1 hour as 33.47 J/g. They concluded that annealed films had a high degree of crystallinity of above 90%. Using their data, the crystallinity of the PVDF-TrFE extruded films in this work is estimated to be about 80 %. The values of Curie transition enthalpy ΔH_c for the extruded films were larger than that of the reference sample, and their Curie transition peaks were sharper; both of which suggest that the lamellae of extruded films are formed by more regular all-trans chains. If polymer chains were less regular, a larger amount of gauche bonds and/or chain kink would exist, thereby making the Curie transition peak broader and shift to lower temperature due to the unavoidable accompany of chain rotation and chain twist during the conformation change from all-trans to trans-gauche.[36]

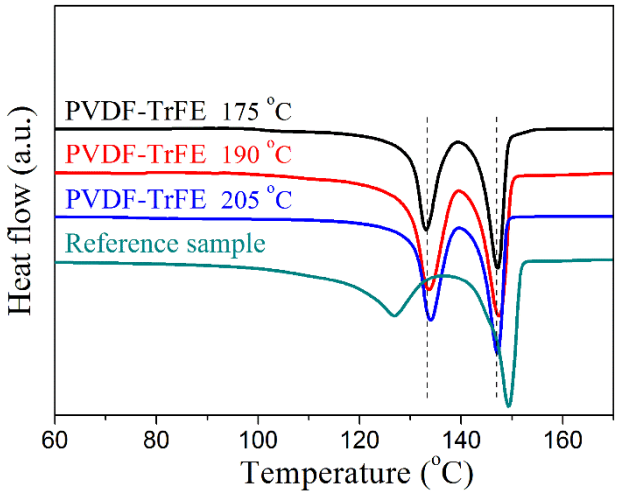

Figure 4 DSC first heating scans of the PVDF-TrFE extruded films. A DSC second heating scan was chosen as a reference to highlight the orientation effect on thermal parameters.

Table 1 Characteristic temperature and thermodynamic parameters from DSC for films extruded at different temperatures and second heating reference samples.

	$*T_c$ (℃)	$*T_m$ (℃)	$*\Delta H_c$ (J/g)	$*\Delta H_f$ (J/g)
Reference	127.1±0.1	149.2±0.1	20.66±0.07	30.11±0.05
Extruded @175 ℃	132.8±0.1	147.4±0.1	25.28±0.18	29.19±0.12
Extruded @190 ℃	134.0±0.1	147.7±0.1	28.93±0.13	28.98±0.15
Extruded @205 ℃	134.2±0.1	147.4±0.1	29.25±0.21	28.91±0.23

$*T_c$: Curie point; T_m: melting temperature; ΔH_c: enthalpy of Curie transition; ΔH_f: fusion enthalpy.

3.4 Ferroelectric properties

Figure 5 shows the ferroelectric properties of the PVDF-TrFE extruded films with a maximum field of 150 kV/mm; the E_c and P_r values are listed with the Current-Electric field (IE) curves (Figure 5a) and Polarization displacement-Electric field (PE) loops (Figure 5b), respectively. The Herman's orientation factor f values were also listed in Figure 5a to emphasize the relationship between preferred orientation and ferroelectric properties. The PE

loops are saturated, which was confirmed by the invariance of the current peak position above a certain maximum applied electric field (~120 kV/mm). The PE loops for the extruded films were nearly square, except for the 175 ℃ extruded films. The larger value of P_r for these films is an artefact arising from current leakage at such a high electric field (150 kV/mm), which is confirmed by the inset in Figure 5a. This current leakage of the 175 ℃ extruded films is induced by the charge accumulation resulted from a slightly larger thickness due to the less extension flow effect during processing. Comparing the ferroelectric data for the 190 and 205 ℃ extruded films, the former ones exhibited lower E_c (and slightly lower P_r), which can be explained by the fact that the 190 ℃ extruded films exhibited easier ferroelectric switching because of the high preferred orientation of their lamella structure. The preferred orientation also influences the dielectric properties of the extruded films (Figure S2). The 190 ℃ extruded films, which had the highest preferred orientation, exhibited the lowest dielectric constant.

From the IE curves, it can be observed that the extruded films exhibited well defined switching current peaks. The position of switching peak for the 190 ℃ extruded PVDF-TrFE films occurs at a lower electric field and a slightly higher maximum current compared to the other extruded films, suggesting easier ferroelectric switching. The value of E_c for the PVDF-TrFE 190 ℃ extruded films was 24 kV/mm, half of the value commonly reported for bulk materials (~50 kV/mm[21,22]). Note that the E_c of the less oriented 175 ℃ extruded films, 52.3 kV/mm, is similar to that typically reported for PVDF-TrFE (films prepared by either hot compression or solution casting).

The theoretical value of the spontaneous polarization P_s of β-PVDF based on a rigid dipole model using the dipole moment and unit cell volume is $P_s = 2\mu_v/abc = 0.13$ C/m^2.[6] The P_s of PVDF-TrFE decreases with increasing molecular ratio of TrFE, which is due to a decrease of the dipole moment and the expansion of the unit cell volume.[22] Using the neutron data for PVDF-TrFE reported by Legrand *et al.*,[16] the average dipole moment of PVDF-TrFE 77/23 mol. % monomer is estimated to be $\mu = \mu_v \times (1-x/2) = 6.2\times10^{-30}$ Cm (where x is equal to the content of TrFE, 0.23); unit cell parameters are a=8.95 Å, b=5.07 Å and c=2.55 Å. Assuming a rigid dipole model, the theoretical value of P_s for PVDF-TrFE 77/23 mol. % is 0.107 C/m^2 which is consistent with the reported results for PVDF-TrFE 75/25 mol. % and PVDF-TrFE 72/28 mol. %.[37,38] Assuming perfect in-plane c-axis orientation and random b-axis orientation, the maximum possible P_r is 0.102 C/m^2 for a fully crystalline material.[6] The maximum

possible P_r value for the extruded films is 0.082 C/m^2 taking 80% crystallinity into calculation. The P_r of the 190 ℃ extruded films (0.078 C/m^2) is close to this estimated value (0.082 C/m^2).

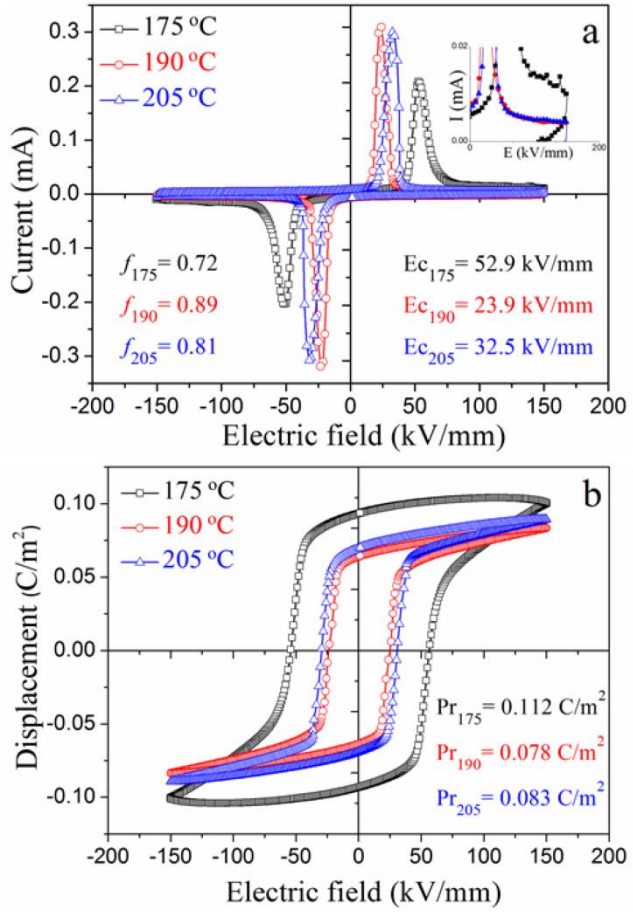

Figure 5 Ferroelectric reversal of PVDF-TrFE extruded films: (a) IE curves; (b) PE loops; the inset in (a) corresponds to IE curves at I < 0.02 mA, 0<E≤150 kV/mm.

The 190 ℃ extruded films were annealed to increase the crystallinity. It was found that the optimum annealing temperature was between the Curie and melting points at 140 ℃ for 24 hours, which is due to the high chain mobility allowing the rearrangement of polymer chains and occurrence of lamellae thickening (Figure 6b bottom right inset SEM). This increased the crystallinity of the PVDF-TrFE films to ~90% (Figure 6a), which improved their ferroelectric properties and P_r value increased to 0.099 C/m^2 with an E_c of 37.9 kV/mm (Figure 6b). The P_r value is close the estimated maximum possible P_r value (0.102 C/m^2) for 100% crystallisation and perfect in-plane c-axis orientation (Figure 7). And due to the hindrance of preferred orientation, f decreased from 0.89 to 0.78 (Figure 6b), the annealed 190 ℃ extruded films show a higher E_c (~38 kV/mm) than as-extruded but still much lower than the

commonly reported values for fully saturated PE loops of ~50 kV/mm. These results compare favourably with the results reported in the literature for free standing copolymer films. For melt compression processed films without poling, the reported P_r values range from 0.058 to 0.065 C/m^2 and E_c from 40 to 50 kV/mm (see Table 2).[22,39] Poling significantly increased P_r to 0.09 C/m^2 for melt compression films.[40] The best previously reported results for a free standing copolymer film are P_r was of 0.11 C/m^2 and E_c of 55 kV/mm for a uniaxially stretched (draw ratio 5) PVDF-TrFE 68/32 mol. % film followed by a two-step annealing process 120 ℃ for 2 hours and 134 ℃ for 2 hours.[21] However, it should be noted that the 0.11 C/m^2 P_r is higher than the rigid model estimated P_s value (0.099 C/m^2), which suggests there might be some current leakage just like 175 ℃ extruded films (Figure 5a).

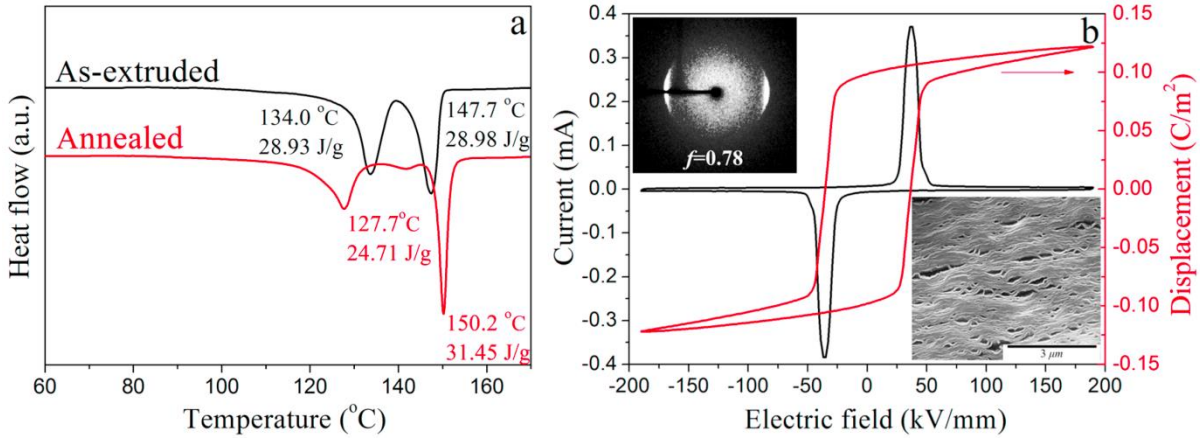

Figure 6 (a) DSC comparison between as-extruded and annealed samples; (b) 2D-WAXD crystalline orientation (top left inset), SEM morphology (bottom right inset) and ferroelectric properties for annealed 190 ℃ extruded films.

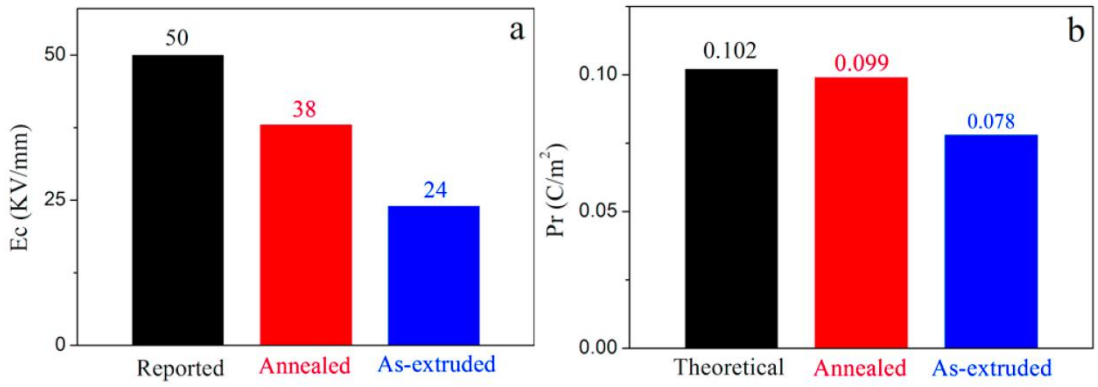

Figure 7 Comparison of ferroelectric properties: (a) E_c values of average reported and PVDF-TrFE 190 ℃ films; (b) P_r values of theoretical limit and PVDF-TrFE 190 ℃ films.

Table 2 Ferroelectric properties of PVDF-TrFE reported in the literature.

Reference	Processing methods	Orientation & thickness	Molecular ratio	E_c (kV/mm)	P_r (C/m^2)	PE loops measurement
This work	Extruded at 190 ℃	Oriented ~15 μm	77/23	**24**	**0.078**	150 kV/mm 10 Hz
	Extruded at 190 ℃; annealed 140 ℃_24 hours	Oriented ~15 μm	77/23	**38**	**0.099**	190 kV/mm 10 Hz
Furukawa *et al.* [41]	Solution cast	Random Not mentioned	55/45	35	0.040	80 kV/mm 300 Hz
Ohigashi *et al.* [42]	Solution cast, uniaxially stretched (five times), annealed 138 ℃_2 hours, and poled	Oriented 10-100 μm	75/25	38	0.10	Not presented
Huang *et al.* [21]	Solution cast, uniaxially stretched (five times), and annealed 120 ℃_2 hours and 134 ℃_2 hours	Oriented ~20 μm	68/32	55	0.11	150 kV/mm 10 Hz
Davis *et al.* [22]	Melt compression	Random ~40 μm	65/25	50	0.058	80 kV/mm 0.0167 Hz
Davis *et al.* [22]	Melt compression	Random ~40 μm	73/27	40	0.065	100 kV/mm 0.0167 Hz
Christie *et al.* [40]	Melt compression; poled at 150 KV/mm	Random ~30 μm	73/27	50	0.090	150 kV/mm 104 Hz

It is well known that the macroscopic nucleation-growth model, which involves domain nucleation and subsequent forward and sideways growth of domains, fits the ferroelectric switching behaviour of most ferroelectrics.[23,24] With regard to PVDF-TrFE, the ferroelectric switching is produced by the rotation of polymer chains[18,24], which is predominantly influenced by the chain packing and the interrelated lamellae crystallites. Figure 8 shows the FTIR spectra for PVDF-TrFE films with different degrees of preferred orientation. The corresponding wavenumber values were listed in Table 3. The characteristic band at about 1170 cm^{-1} is mainly assigned to the asymmetric stretching of the CF_2 group ($\nu_a(CF_2)$).[43] The

positive contribution of the wagging vibration of CH_2 group ($\omega(CH_2)$) and the negative contribution of asymmetric stretching of CC group ($v_a(CC)$) are associated with the formation of the characteristic band at about 1400 cm^{-1}.[43] The 190 ℃ extruded films exhibited a highest wavenumber (1176 cm^{-1}) of $v_a(CF_2)$ band and a lowest wavenumber (1392 cm^{-1}) of $\omega(CH_2)$-$v_a(CC)$ band (Table 3). On the basis of Hooke's law, the vibration frequency is determined by the force constant and the atom mass. Therefore the highest frequency of $v_a(CF_2)$ and lowest frequency of $\omega(CH_2)$-$v_a(CC)$ bands indicate the largest force constant, which suggests that the strongest bonds exist between C-F and C-C. Polymer chains align nearly perfectly along the extrusion direction in the 190 ℃ extruded films. The parallel chain packing enables the F atoms in one molecular chain be attracted to the H atoms in its neighbouring chain, thereby generating the intermolecular dipole-dipole interaction. Such intermolecular interaction gives rise to a close chain packing. This is in line with the perfect alignment of lamellae crystallites in the 190 ℃ extruded films. More ordered chain packing significantly decreases the pinning sites[24,25] for domain walls in PVDF-TrFE, which promotes the ferroelectric polarization reversal and further reduces the coercive field.

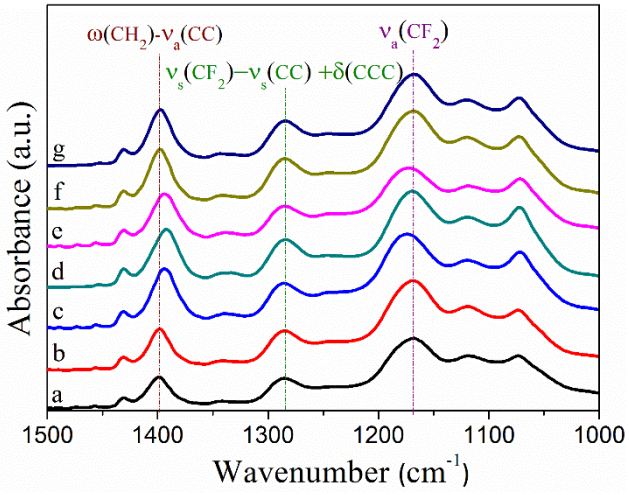

Figure 8 FTIR spectra of the PVDF-TrFE films with different degrees of preferred orientation: (a) 170 °C; (b) 175 °C; (c) 190 °C; (d) 190 °C annealed; (e) 205 °C; (f) 210 °C; (g) hot pressed films with random orientation.

Table 3 Assignment and position of the characteristic bands for PVDF-TrFE films with different degrees of preferred orientation

	Bands assignment and position (cm^{-1})		
	*$\omega(CH_2)$-$\nu_a(CC)$	*$\nu_s(CF_2)$-$\nu_s(CC)+\delta(CCC)$	*$\nu_a(CF_2)$
170 °C films	1398	1284	1168
175 °C films	1398	1284	1169
190 °C films	1392	1284	1176
190 °C; annealed films	1393	1284	1169
205 °C films	1394	1284	1174
210 °C films	1398	1284	1168
Hot pressed films	1398	1284	1168

*ω, wagging vibration; ν_a, asymmetric stretching vibration; ν_s, symmetric stretching vibration; δ, bending vibration

4. Conclusions

Highly crystalline and oriented PVDF-TrFE films can be produced by melt extrusion, with the polymer chain axis along extrusion direction. The crystalline structure and orientation level can be controlled by changing the extrusion temperature. The optimum extrusion temperature was found to be 190 ℃. The 190 ℃ extruded PVDF-TrFE films exhibited a well stacked edge-on lamella structure with remarkable ferroelectric properties. The coercive field was 23.9 kV/mm and the remnant polarization (0.078 C/m^2) was close to the estimated remnant polarization value assuming perfect in-plane c-axis orientation and 80% crystallinity (0.082 C/m^2). After annealing at 140 ℃ the crystallinity of the films was increased (~90%) and the ferroelectric properties further improved with P_r of 0.099 C/m^2 and E_c of 37.9 kV/mm. This work demonstrates for the first time the produce of highly aligned ferroelectric copolymer films with pronounced ferroelectric properties, with a significantly low coercive field and high remnant polarization, using extrusion, a highly scalable processing route.

Acknowledgements:

Nan Meng would like to thank the China Scholarship Council (CSC) for the financial support.

Prof. *M.J. Reece* would like to acknowledge the support of Sunchon National University, South Korea, through the BK21+ programme.

Reference

1. Y. Yuan, T. J. Reece, P. Sharma, S. Poddar, S. Ducharme, A. Gruverman, Y. Yang, J. Huang. *Nat Mater* **2011**, *10*, 296-302.
2. P. M. Richardson, A. M. Voice, I. M. Ward. *Polymer* **2016**, *97*, 69-79.
3. D. Kim, D.-Y. Khang. *Polymer* **2014**, *55*, 2491-2495.
4. L. Yao, D. Wang, P. Hu, B.-Z. Han, Z.-M. Dang. *Advanced Materials Interfaces* 2016, *3*, 1600016.
5. A. V. Shirinov, W. K. Schomburg. *Sensors and Actuators A: Physical* **2008**, *142*, 48-55.
6. T. Furukawa. *Phase Transit* **1989**, *18*, 143-211.
7. O. R. Hughes. *Journal of Polymer Science Part B: Polymer Physics* **2007**, *45*, 3207-3214.
8. R. Hasegawa, Kobayashi, M., Tadokoro, H. *Polymer Journal* **1972**, *3*, 591-599.
9. A. J. Lovinger. *Science* **1983**, *220*, 1115-1121.
10. T. Yagi, M. Tatemoto, J.-i. Sako. *Polym J* **1980**, *12*, 209-223.
11. T. Furukawa, M. Ohuchi, A. Chiba, M. Date. *Macromolecules* **1984**, *17*, 1384-1390.
12. T. Furukawa, G. E. Johnson. *J Appl Phys* **1981**, *52*, 940-943.
13. G. T. Davis, T. Furukawa, A. J. Lovinger, M. G. Broadhurst. *Macromolecules* **1982**, *15*, 329-333.
14. K. Tashiro, K. Takano, M. Kobayashi, Y. Chatani, H. Tadokoro. *Polymer* **1984**, *25*, 195-208.
15. F. Ishii, A. Odajima, H. Ohigashi. *Polym J* **1983**, *15*, 875-882.
16. E. Bellet-Amalric, J. F. Legrand. *Eur. Phys. J. B* **1998**, *3*, 225-236.
17. M. Tamura, S. Hagiwara, S. Matsumoto, N. Ono. *J Appl Phys* **1977**, *48*, 513-521.
18. R. G. Kepler. *Annual Review of Physical Chemistry* **1978**, *29*, 497-518.
19. K. B. Chong, F. Guiu, M. J. Reece. *J Appl Phys* **2008**, *103*, 014101.
20. S. Ducharme, V. M. Fridkin, A. V. Bune, S. P. Palto, L. M. Blinov, N. N. Petukhova, S. G. Yudin. *Physical Review Letters* **2000**, *84*, 175-178.
21. C. Huang, R. Klein, F. Xia, H. Li, Q. M. Zhang, F. Bauer, Z. Y. Cheng. *Dielectrics and Electrical Insulation, IEEE Transactions on* **2004**, *11*, 299-311.
22. G. T. Davis, M. G. Broadhurst, A. J. Lovinger, T. Furukawa. *Ferroelectrics* **1984**, *57*, 73-84.
23. T. Furukawa. *Advances in Colloid and Interface Science* **1997**, *71–72*, 183-208.
24. W. J. Hu, D.-M. Juo, L. You, J. Wang, Y.-C. Chen, Y.-H. Chu, T. Wu. *Scientific Reports* **2014**, *4*, 4772.
25. Y. Tan, J. Zhang, Y. Wu, C. Wang, V. Koval, B. Shi, H. Ye, R. McKinnon, G. Viola, H. Yan. *Scientific Reports* **2015**, *5*, 9953.
26. E. S. Sherman. *Polymer Engineering & Science* **1984**, *24*, 895-907.
27. A. Prasad, R. Shroff, S. Rane, G. Beaucage. *Polymer* **2001**, *42*, 3103-3113.
28. A. Keller, M. J. Machin. *Journal of Macromolecular Science, Part B* **1967**, *1*, 41-91.
29. T. Kanaya, I. A. Polec, T. Fujiwara, R. Inoue, K. Nishida, T. Matsuura, H. Ogawa, N. Ohta. *Macromolecules* **2013**, *46*, 3031-3036.
30. R. T. Chen, C. K. Saw, M. G. Jamieson, T. R. Aversa, R. W. Callahan. *J Appl Polym Sci* **1994**, *53*, 471-483.
31. Z. Bashir, J. A. Odell, A. Keller. *J Mater Sci* **1986**, *21*, 3993-4002.
32. L. Balzano, S. Rastogi, G. Peters. *Macromolecules* **2011**, *44*, 2926-2933.
33. A. J. Lovinger, G. T. Davis, T. Furukawa, M. G. Broadhurst. *Macromolecules* **1982**, *15*, 323-328.
34. N. Shingne, M. Geuss, B. Hartmann-Azanza, M. Steinhart, T. Thurn-Albrecht. *Polymer* **2013**, *54*, 2737-2744.

35. C. Chen, Q. Jiang, X. Wei, I. Abrahams, H. Yan, M. J. Reece. *J Am Ceram Soc* **2014**, *97*, 3624-3630.
36. K. Koga, H. Ohigashi. *J Appl Phys* **1986**, *59*, 2142-2150.
37. O. Hiroji, K. Keiko. *Japanese Journal of Applied Physics* **1982**, *21*, L455.
38. Y. J. Shin, R. H. Kim, H. J. Jung, S. J. Kang, Y. J. Park, I. Bae, C. Park. *ACS Applied Materials & Interfaces* **2011**, *3*, 4736-4743.
39. T. Furukawa, A. J. Lovinger, G. T. Davis, M. G. Broadhurst. *Macromolecules* **1983**, *16*, 1885-1890.
40. M. C. Christie, J. I. Scheinbeim, B. A. Newman. *Journal of Polymer Science Part B: Polymer Physics* **1997**, *35*, 2671-2679.
41. T. Furukawa, G. E. Johnson, H. E. Bair, Y. Tajitsu, A. Chiba, E. Fukada. *Ferroelectrics* **1981**, *32*, 61-67.
42. H. Ohigashi, K. Omote, T. Gomyo. *Appl Phys Lett* **1995**, *66*, 3281-3283.
43. M. Kobayashi, K. Tashiro, H. Tadokoro. *Macromolecules* **1975**, *8*, 158-171.

Supporting Information

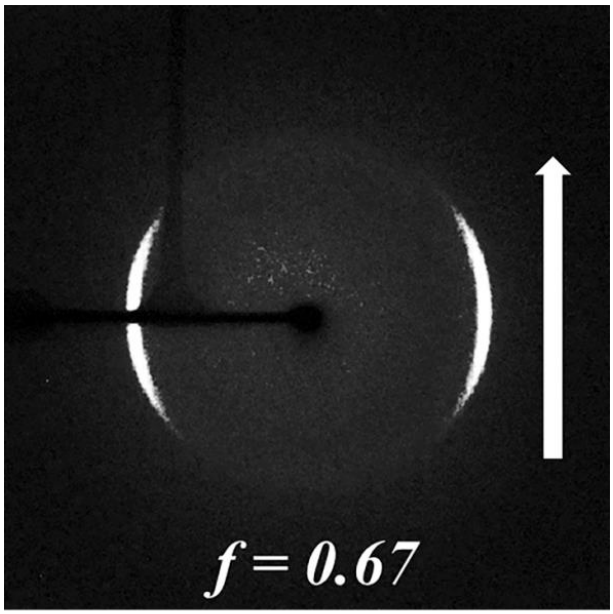

Figure S1 *2D WAXD for extruded PVDF-TrFE 51/49 mol. % films.*

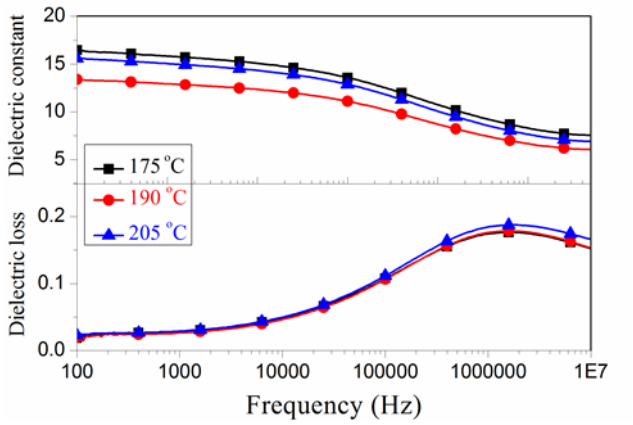

Figure S2 *The frequency dependence of dielectric permittivity for films extruded at different temperatures.*